

THE SOLAR NEIGHBORHOOD. VII. DISCOVERY AND CHARACTERIZATION OF NEARBY MULTIPLES IN THE CTIO PARALLAX INVESTIGATION

WEI-CHUN JAO,¹ TODD J. HENRY,¹ AND JOHN P. SUBASAVAGE¹

Department of Physics and Astronomy, Georgia State University, Atlanta, GA 30303-3083;
jao@chara.gsu.edu, thenry@chara.gsu.edu, subasavage@chara.gsu.edu

JACOB L. BEAN^{1,2}

School of Physics, Georgia Institute of Technology, Atlanta, GA 30332-0430; bean@astro.as.utexas.edu

EDGARDO COSTA¹

Departamento de Astronomía, Universidad de Chile, Casilla 36-D, Santiago, Chile; costa@das.uchile.cl

PHILIP A. IANNA¹

Department of Astronomy, University of Virginia, Charlottesville, VA 22903-0818; pai@virginia.edu

AND

RENÉ A. MÉNDEZ¹

European Southern Observatory, Casilla 19001, Santiago 19, Chile; rmendez@eso.org

Received 2002 September 3; accepted 2002 October 7

ABSTRACT

We report the discovery of eight new multiple star systems among 191 stellar systems targeted for parallax determinations in the RECONS (Research Consortium on Nearby Stars) southern parallax program, CTIOPI (Cerro Tololo Inter-American Observatory Parallax Investigation). The eight new companions have separations of 1".42 to 14".90 and instrumental magnitude differences at *VRI* of 0.06–6.07 mag. Orbital motion has not been detected in any of these systems. These new companions increase the multiplicity fraction of this sample, made up primarily of nearby (less than 25 pc) M dwarfs, to 15%. Comparison with samples that have been more completely scrutinized for companions indicates that probably only half of all multiples have so far been discovered. Given the large number of frames acquired for the astrometric series, the eight new systems and 16 known multiples have been searched for variability at *VRI* during the 3 year duration of CTIOPI. A flare has been detected in the secondary of the RX J1132–264 system, while at least one component in the GJ 2006 system is a probable long-term variable. Variables were detected in only 9% of the systems searched, primarily as a result of the restrictive 0.05 mag threshold required for variability confirmation.

Key words: astrometry — binaries: close — stars: low-mass, brown dwarfs — stars: statistics — stars: variables: other — surveys

1. INTRODUCTION

The solar vicinity provides astronomers with the foundation of stellar astronomy and our understanding of the population of the Galaxy and holds a special attraction for the general public. A wide range of astrophysical problems are addressed by studying the nearby star population, including star formation, evolution, mass transfer, the stellar luminosity function, Galactic dynamics, and searches for planetary systems. All of these problems rely, at least in part, on an accurate census of single versus multiple stars. A recent nearby-star census indicates that ∼35% of stellar systems are missing within 10 pc of the Sun (Henry et al. 1997), and a similar (although not as well defined) problem exists for the census of companions. Undoubtedly, many missing companions have not yet been revealed.

The RECONS (Research Consortium on Nearby Stars) team is currently carrying out a southern parallax survey

known as CTIOPI (Cerro Tololo Inter-American Observatory Parallax Investigation). The purpose of CTIOPI is to discover nearby red, brown, and white dwarfs that are unidentified in the solar neighborhood. The goal is to discover 150 new southern star systems by determining trigonometric parallaxes accurate to 3 mas. This is a primary research effort of the NStars (Nearby Stars) project, a joint NASA/NSF effort to discover and characterize all stellar systems within 25 pc. Here we report on a comprehensive search for new companions to 209 stars in 191 systems targeted at the 0.9 m telescope.

Investigations of stellar multiplicity in the solar neighborhood have been carried out using a wide range of survey techniques, including searches for astrometric perturbations from parallax frames (van de Kamp 1986), radial velocity studies (Abt & Levy 1976; Marcy & Benitz 1989; Duquennoy & Mayor 1991; Delfosse et al. 1999), infrared speckle imaging (Henry & McCarthy 1990; Henry 1991; Leinert et al. 1997), optical imaging (van Biesbroeck 1961), deep infrared imaging (Skrutskie, Forrest, & Shure 1989; Simons et al. 1996; McCarthy, Zuckerman, & Becklin 2001; Hinz et al. 2002), and by the careful compilations of wide multiples (Poveda et al. 1994). This paper reports an additional effort to identify companions at modest separations, 2"–20", using frames taken during a southern sky astrometric program

¹ Visiting Astronomer, Cerro Tololo Inter-American Observatory. CTIO is operated by the Association of Universities for Research in Astronomy, Inc., under cooperative agreement with the National Science Foundation.

² Current address: Department of Astronomy, University of Texas at Austin, Austin, TX 78712.

that targets a large sample of known and probable nearby stars.

2. SAMPLE AND OBSERVATIONS

Most of the 209 target stars were selected for CTIOPI because available astrometric (e.g., high proper motion), photometric, or spectroscopic data indicated that they might be closer than 25 pc. Other than eight calibration stars and 22 stars that are being observed to improve poor parallaxes ($\sigma_\pi > 10$ mas now), very few of the targets have any trigonometric parallax measurements. Roughly 95% of the stars are red dwarfs, with the remainder being a mixture of white dwarfs and a small fraction of stars that are probably distant giants. The targets and their coordinates are listed in Table 1.

CTIOPI uses the 0.9 m and 1.5 m CTIO telescopes in a long-term observing program as part of the NOAO Surveys initiative. Observations used to discover and characterize the new multiple systems reported here occurred during the 3 yr period from 1999 August through 2002 July. The current work includes stars observed at the 0.9 m, which is equipped with a 2048×2048 Tektronix CCD camera with $0.^{\prime\prime}401 \text{ pixel}^{-1}$ plate scale (see next section). All observations were made using the central quarter of the chip, yielding a $6.^{\circ}8$ square field of view, through V_J , R_C , and I_C filters.

Bias frames and dome flats were taken at the beginning of each night. Observations were usually taken when a target star was within 30 minutes of transit, in order to minimize corrections required for differential refraction. The current study benefits from this observing protocol because no corrections need to be applied to compensate for the varying centroid shifts for stars of different colors. At each epoch, a sequential set of 5–10 astrometric frames with exposures of 30–1200 s is typically taken. The filter for astrometry frames (listed in Table 1) is chosen based on the best combination of science and reference star counts and was applied throughout the observing program. Suitable reference stars were selected to have a signal-to-noise ratio $S/N > 100$, which allows for accurate centroiding, and so they were well distributed around the target star. Photometry frames in the other two filters are often taken after the astrometric frames.

3. DATA REDUCTION AND ANALYSIS: ASTROMETRY

The raw data were reduced by using the standard Image Reduction and Analysis Facility (IRAF) tasks ZEROCOMBINE, FLATCOMBINE, and CCDPROC. The preliminary centroids of science and reference stars are tagged using the IRAF RIMCURSOR task and then imported to SExtractor (Bertin & Arnouts 1996), which is used to determine the peak counts, total fluxes, and centroids for targets and selected reference stars. Five to 15 reference stars are typically chosen for each target field in order to determine accurate astrometric quantities. In the present study, the four relevant quantities are the separation between components, position angle of the separation, proper motion, and position angle of the proper motion.

3.1. Plate Scale

CTIOPI astrometry frames were used first to determine an accurate plate scale for the Tek 2K CCD imager No. 3

on the CTIO 0.9 m. Eleven parallax fields were selected that had three or four pairs of stars with separations greater than half the size of the used portion of the CCD (the central quarter). Each of the six or eight stars per field was required to have $S/N > 1000$ and to have no nearby sources, to ensure that accurate centroids could be obtained. In order to minimize the effect of differential refraction, all of the selected frames were taken within $4'$ of the meridian in right ascension, as well as within 5° of the zenith in declination.

A total of 40 star pairs were used to determine the plate scale. Coordinates with right ascension accurate to thousandths of a second of time and declination to hundredths of an arcsecond were extracted from the Guide Star Catalog 2 using SkyCat (Albrecht et al. 1997). For each star pair, the differences in right ascension and declination were determined in radians, and the vector separation was calculated along a great-circle line via standard trigonometric functions. The resultant radian values were then converted to separations in arcseconds and compared with the separations in pixels determined using SExtractor on the CCD frames. The final plate scale determined was $0.^{\prime\prime}4012 \pm 0.^{\prime\prime}0003 \text{ pixel}^{-1}$. This is slightly, yet significantly, different from the accepted value for the camera on the CTIO 0.9 m, $0.^{\prime\prime}396 \text{ pixel}^{-1}$.

3.2. Companion Search

A comprehensive search for companions to 209 stars in 191 stellar systems was carried out using the CTIOPI astrometry images. Images were examined for objects located within a $20''$ radius of each target star using the contour capability in the IRAF package IMEXAMINE. Typically, 1–10 sources were discovered per target. Most potential companions were quickly refuted by comparing first- and second-epoch Digitized Sky Survey (DSS) images and discovering proper motions inconsistent with the target stars. After culling the unrelated sources, eight potential new companions remained (listed in order of right ascension): GJ 2022C, LHS 193B, LHS 1749B, LHS 225B, LHS 300B, RX J1132–264B, GJ 1226B, and LTT 7419B. Finder charts from CTIOPI frames for these systems are shown in Figure 1.

In order to characterize the search sensitivity, each frame was evaluated for image quality. Figure 2 shows a histogram of the full-width at half-maximum values (FWHM; see Table 1) for the objects investigated, separated by the filters used for the observations. Most of the stars (90%) were examined using V or R images. The FWHM values were determined using a radial profile Moffat fit in IRAF's IMEXAMINE. When possible, frames were chosen that had FWHM better than $1.^{\prime\prime}20$ (3 pixels). For a modest fraction of the stars (12%), images with somewhat poorer FWHM were used because sharper images were not available. The mean FWHM value for the 209 targets searched is $1.^{\prime\prime}09$.

The CTIOPI program has resulted in at least a factor of 5 improvement in resolution over DSS, thereby enabling the detection of closer and fainter companions. The DSS image plate scales are $1.^{\prime\prime}7 \text{ pixel}^{-1}$ for the first generation and $1.^{\prime\prime}0 \text{ pixel}^{-1}$ for the second generation, determined by using information in the FITS headers delivered from DSS. Examination of ~ 100 stellar sources in 20 second-generation DSS fields with CTIOPI targets reveals an average FWHM value of $5.^{\prime\prime}64$ for stars that were not saturated. For targets that were saturated, which includes most of the stars

TABLE 1
STARS EVALUATED FOR MULTIPLICITY

Object Name	R.A. (J2000.0)	Decl. (J2000.0)	Ref.	Fil.	FHWM (arcsec)	Object Name	R.A. (J2000.0)	Decl. (J2000.0)	Ref.	Fil.	FHWM (arcsec)
GJ 1001	00 04 36	-40 44 03	B	R	1.08	LHS 1731	05 03 20	-17 22 25	T	V	1.18
LTT 57	00 08 20	-57 05 51	S	V	1.06	BD -21°1074A	05 06 50	-21 35 09	T	V	1.05
GJ 131-026	00 08 54	+20 50 18	S	V	1.12	BD -21°1074 BC	05 11 51	-29 39 05	Sch ^b	R	1.42
LHS 1050	00 15 49	+13 33 22	B	V	1.19	APMPM J0512-2939	05 15 37	-22 00 11	Del	R	1.06
G266-039A	00 19 37	-28 09 48	B	V	1.21	DENIS J0515-2200	05 15 47	-31 17 46	B	V	1.08
G266-039B	00 19 37	-28 09 48	B	V	1.20	LHS 1748	05 16 01	-72 14 15	B	V	1.33
GJ 2005 ABC	00 24 44	-27 08 26	B	R	1.02	LHS 1749 AB	05 37 39	-61 55 07	S	R	0.97
GJ 2006A	00 27 51	-32 33 06	S	V	1.04	WT 178	05 42 13	-05 27 57	B	I	1.08
GJ 2006B	00 27 51	-32 33 06	S	V	1.01	LHS 1777	05 43 46	-41 08 05	Sch	V	1.18
GJ 2012	00 41 26	-22 21 04	B	R	1.09	APMPM 0544-4108	06 00 04	+02 42 23	S	V	1.11
LHS 124	00 49 29	-61 02 34	B	V	1.36	G099-049	06 02 23	-20 19 46	B	R	1.05
GJ 2014	00 50 00	-26 25 00	S	R	0.99	LHS 1807	06 10 53	-43 24 20	B	V	1.20
LHS 125	00 50 17	-39 30 11	B	R	1.20	GT 1088	06 35 45	-55 31 30	Del	R	1.14
GJ 1025	01 00 56	-04 26 57	B	V	1.03	DENIS J0635-5531	06 43 42	-26 25 00	S	R	1.19
GJ 54	01 10 23	-67 26 42	T	V	1.19	LTT 2631	07 04 46	-38 36 09	B	V	1.11
LP 467-016	01 11 25	+15 26 24	S	R	1.17	LHS 225 AB	07 09 37	-57 03 45	Sch	R	1.04
DENIS J0113-5429	01 13 16	-54 29 14	Del	S	1.03	APMPM J0710-5704	07 36 12	-51 55 23	B	V	0.86
GJ 2022 AC	01 24 28	-33 55 12	S	R	1.05	LHS 1932	07 36 25	+07 04 36	S	R	0.98
GJ 2022B	01 24 28	-33 55 12	S	R	1.05	G089-032 AB	07 54 55	-29 20 58	B	R	1.34
GJ 2023	01 29 54	-30 56 00	S	V	1.08	LHS 1955 AB	07 56 14	-67 05 19	S	V	1.18
LHS 145	01 43 01	-67 18 35	B	V	1.08	WT 233	08 12 41	-21 33 08	B	V	0.95
LHS 1302	01 51 04	-06 07 04	B	R	1.28	GT 300	08 27 12	-44 59 23	B	V	0.99
G274-138A	02 02 19	-26 33 19	S	I	0.96	LHS 2010	08 53 57	-24 46 58	B	I	0.91
G274-138B	02 02 19	-26 33 54	S	I	0.96	LHS 2067 (A)	09 16 31	-62 04 42	B	R	0.89
LHS 1351	02 11 18	-63 13 43	B	V	1.17	LHS 2068 (B) ^a	09 17 06	-77 49 25	B	V	1.15
LHS 1358	02 12 55	+00 00 16	B	R	1.11	LHS 2071	09 42 46	-68 53 09	B	V	0.86
APMPM J0237-5928	02 36 33	-59 28 05	Sch	R	1.10	G041-014 ABC	09 43 46	-31 13 27	B	R	1.13
GJ 1050	02 39 51	-34 08 01	B	V	1.14	GJ 1118	09 59 05	-07 03 03	B	R	1.13
LHS 1429	02 39 56	+06 46 31	B	R	1.07	LHS 2106	09 44 29	-73 58 39	S	I	0.97
LHS 158	02 42 02	-44 31 01	B	I	1.19	LHS 2122	09 44 47	-18 12 49	B	V	0.91
LTT 1323	02 42 56	-38 56 14	B	V	1.23	GJ 1123	09 53 55	+20 56 45	B	R	1.20
LP 993-115 (A)	02 45 14	-43 44 02	S	V	1.01	GJ 1128	10 05 55	-67 21 31	S	I	0.82
LP 993-116 (B) ^a	02 45 14	-43 44 02	S	V	1.19	WT 248	10 12 02	-18 43 34	S	I	1.30
LHS 164	03 01 41	-34 57 57	B	V	1.23	WT 272	10 14 52	-47 09 27	B	R	1.00
LHS 164	03 01 51	-16 35 36	H	V	1.11	WT 244	10 19 51	-41 48 45	B	V	0.91
LP 771-095 (A)	03 01 51	-16 35 31	S	V	1.18	GJ 1129	10 19 54	-41 49 00	B	V	0.94
LP 771-096 (BC) ^a	03 04 04	-20 22 43	B	V	1.16	LHS 2206	10 30 35	-10 02 12	S	R	1.15
LHS 1491	03 07 58	-28 13 17	T	R	0.96	WT 1827	10 43 09	-09 13 00	S	V	0.97
HIP 14559	03 12 42	-54 06 54	S	R	1.34	LHS 288	10 44 32	-61 11 42	B	R	1.16
L227-140	03 34 40	-04 50 34	B	R	1.19	DENIS J048-3956	10 48 15	-39 56 06	Del	I	0.93
LHS 1561	03 36 00	-44 30 47	B	R	1.18	LHS 2528	10 55 35	-09 20 27	B	R	0.92
GJ 1061	04 11 27	-44 18 10	S	R	1.16	LHS 2335	10 58 35	-31 08 39	B	V	1.09
G007-034	04 17 18	+08 49 37	S	R	1.17	LHS 300 AB	11 11 14	-41 04 35	B	R	0.93
LHS 1610	03 52 42	+17 01 02	B	V	1.07	LHS 2401	11 23 57	-18 21 48	B	V	0.89
DENIS J0354-1437	03 54 20	-14 37 39	Del	I	1.16	WD 1126-185	11 29 19	+18 16 40	S	R	0.99
LHS 1630	04 07 21	-24 29 13	B	V	0.85	LHS 306	11 31 08	-14 57 23	B	R	0.99
GJ 1068	04 10 27	-53 36 10	B	R	1.04	RX J1132-264A	11 32 42	-26 51 55	S	V	1.32
WT 135	04 11 27	-27 21 00	S	V	1.02	RX J1132-264B	11 32 42	-26 51 55	S	V	1.34
G007-034	04 17 18	+08 49 37	S	R	1.05	GJ 1147	11 38 25	-41 22 33	B	V	1.11
LHS 193A	04 32 29	-38 59 48	B	V	1.01	GJ 438	11 43 20	-51 49 16	B	V	1.18
LHS 193B	04 32 29	-38 59 48	B	V	1.02						
LTT 2043 (A)	04 36 36	-27 21 00	S	V	1.03						
LTT 2044 (B) ^a	04 36 36	-27 21 00	S	V	1.03						
G039-029	04 38 13	+28 13 00	S	V	1.38						
LHS 1723	05 01 58	-06 56 47	B	V	1.03						
LP 476-207 ABC	05 01 59	+09 58 59	H	V	1.39						

TABLE 1—Continued

Object Name	R.A. (J2000.0)	Decl. (J2000.0)	Ref.	Fil.	FWHM (arcsec)	Object Name	R.A. (J2000.0)	Decl. (J2000.0)	Ref.	Fil.	FWHM (arcsec)
GJ 440.	11 45 43	-64 50 29	B	V	0.97	LTT 6962.....	17 33 21	-64 19 40	S	R	1.13
CE 440-087	11 47 51	-28 49 41	S	I	0.84	GJ 2130 AC	17 46 13	-32 06 10	H	V	0.97
CE 440-139	12 03 28	-29 23 00	S	R	0.97	GJ 2130 B	17 46 15	-32 06 06	H	V	0.97
WT 1928	12 08 08	-32 06 33	S	V	0.94	LHS 456.....	17 50 55	-56 34 54	B	V	1.21
LHS 2520.	12 10 06	-15 04 18	B	V	1.04	LTT 7138	17 57 22	-41 59 18	S	V	1.00
GJ 1157	12 23 02	-46 37 10	B	V	0.87	LHS 3367	18 12 36	-79 11 52	B	I	1.13
GJ 465.	12 24 53	-18 14 32	T	V	0.85	GJ 1226 AB.....	18 20 57	-01 02 59	B	I	0.86
LHS 327	12 25 51	-24 33 19	B	R	0.91	WT 562	18 26 20	-65 47 11	S	I	1.13
GJ 1158	12 29 35	-55 59 39	B	R	0.98	GJ 729	18 49 49	-23 50 10	H	V	1.13
LHS 2567 (A)	12 29 54	-05 27 24	B	R	1.01	LHS 3413	18 49 51	-57 26 51	B	R	1.12
LHS 2568 (B) ^a	12 29 55	-05 27 22	B	R	1.05	LTT 7119 AB	18 49 53	-33 22 46	S	V	1.31
LHS 337	12 38 49	-38 22 56	B	R	1.26	LHS 3443	19 13 08	-39 01 55	B	V	0.96
LHS 2634	12 47 10	-03 34 18	B	V	0.95	GJ 754	19 20 48	-45 33 32	B	V	1.12
WT 1962	12 59 53	-07 30 45	S	I	1.15	LHS 475	19 20 55	-82 33 15	B	V	1.16
LHS 346	13 09 22	-40 09 29	B	V	0.87	LHS 762	19 34 37	-62 50 40	B	V	1.15
LHS 347	13 10 02	+22 30 04	B	R	0.98	LHS 3484	19 47 05	-71 05 33	B	R	1.34
ER 2.	13 13 14	-41 30 40	S	V	1.20	GJ 7813	20 10 12	-21 46 00	S	V	0.96
LTT 5066	13 13 36	-32 27 00	S	R	1.10	GJ 1252	20 27 42	-56 27 27	B	R	1.07
LHS 2718	13 20 04	-35 24 46	B	V	1.02	GJ 1251	20 28 04	-76 40 16	B	R	1.09
LHS 2729	13 23 38	-25 54 46	B	R	0.96	LHS 3583	20 46 38	-81 43 15	B	V	1.36
GI 65-008	13 31 47	+29 16 37	S	R	1.07	LHS 500 (B) ^a	20 55 37	-14 03 36	B	V	1.03
LHS 2836.	13 59 11	-19 50 04	B	V	1.08	LHS 501 (A).....	20 55 38	-14 02 09	B	V	0.98
WT 460	14 12 03	-41 32 15	S	I	1.12	LHS 3615	21 03 22	-50 22 54	B	R	1.17
GI 545.	14 20 08	-09 37 15	B	V	1.05	APMPM J2109-4003	21 08 31	-40 03 46	Sch ^b	R	1.47
LHS 2899	14 21 15	-01 07 22	B	V	1.03	APMPM J2127-3844	21 27 04	-38 44 46	Sch ^b	R	1.09
APMPM J1425-2945	14 25 03	-29 44 45	Sch ^b	R	0.97	LTT 8526	21 28 19	-22 18 30	S	V	0.99
Proxima Cen	14 29 43	-62 40 46	H	V	1.08	LHS 510	21 30 48	-40 42 31	B	R	1.11
LHS 2935.	14 32 09	+08 11 30	B	R	1.09	WT 795	21 36 23	-44 00 27	S	V	1.16
GI 555.	14 34 17	-12 31 10	T	V	1.16	LHS 512	21 38 44	-33 39 55	B	V	1.03
LHS 382.	14 50 42	-16 56 35	B	I	1.11	LHS 3719	21 49 26	-63 06 53	B	V	1.12
LHS 3001 (A)	14 56 27	+17 54 59	B	I	1.06	LHS 3738 (B) ^a	22 27 59	-32 26 27	B	R	0.98
LHS 3002 (B) ^a	14 56 28	+17 55 07	B	R	1.01	LHS 3739 (A).....	21 58 50	-32 28 20	B	R	0.97
GI 581.	15 19 27	-07 43 20	T	V	1.15	LHS 3746	22 02 30	-37 04 55	B	V	0.89
LHS 3080.	15 31 54	+28 51 08	B	R	1.35	WT 870	22 06 43	-44 57 58	S	R	1.11
LHS 406.	15 43 19	-20 15 35	B	R	1.16	RX J2227-0111	22 27 48	-01 13 33	S	I	1.41
LHS 3124.	15 51 22	+29 31 06	B	V	1.15	LHS 521	22 27 59	-30 09 35	B	R	1.06
LHS 3147.	16 02 24	-25 05 59	B	R	1.11	LHS 8336	22 38 03	-65 50 09	B	R	1.00
LHS 3167.	16 13 06	-70 09 12	B	R	1.09	LTT 9123 (A).....	22 38 25	-29 21 13	S	V	1.06
LHS 3169.	16 14 22	-28 30 38	B	V	1.15	LTT 9124 (B) ^a	22 38 25	-29 21 13	S	V	1.03
LHS 3218.	16 35 25	-27 18 57	B	R	0.93	GJ 1275	22 45 25	-60 03 50	B	V	1.32
LHS 423.	16 35 40	-30 51 20	B	V	1.13	GI 1281	23 10 42	-19 13 36	B	V	1.14
GI 633.	16 40 45	-45 59 59	B	V	1.05	LHS 3909	23 12 11	-14 06 13	B	R	1.08
GI 2122 AB.	16 45 18	-38 48 21	S	V	1.34	LHS 539	23 15 52	-37 33 31	B	R	1.06
GI 69-029.	16 50 57	+22 26 48	S	R	1.19	LHS 3925	23 17 50	-48 18 50	B	R	1.34
HIP 82724.	16 54 32	-62 24 01	H	V	1.00	LHS 547	23 36 53	-36 28 54	B	V	1.10
HIP 82725.	16 54 33	-62 24 12	H	V	1.00	LHS 4009	23 45 31	-16 10 19	B	R	1.13
GI 1207.	16 57 06	-04 20 57	B	V	1.04	LHS 4021	23 50 32	-09 33 33	B	V	1.03
LHS 440.	17 18 29	-43 25 34	B	R	1.05	LTT 9828	23 59 46	-44 04 18	S	V	1.19
LTT 6933.	17 28 08	-62 27 16	B	R	0.94	LHS 4058	23 59 51	-34 06 42	B	V	1.13
LHS 3295.	17 29 26	-80 08 57	B	V	1.18						

Notes.—Units of right ascension are hours, minutes, and seconds, and units of declination are degrees, arcminutes, and arcseconds. Coordinate references are as follows: (B) Bakos, Sahu, & Németh 2002; (D) X. Delfosse (1999, private communication); (H) *Hipparcos* database; (S) SIMBAD database; (T) Tycho database.

^a Hereafter referred to as component(s) “B” (and “C”) in the system.

^b Coordinates from R-D. Scholz (1999, private communication).

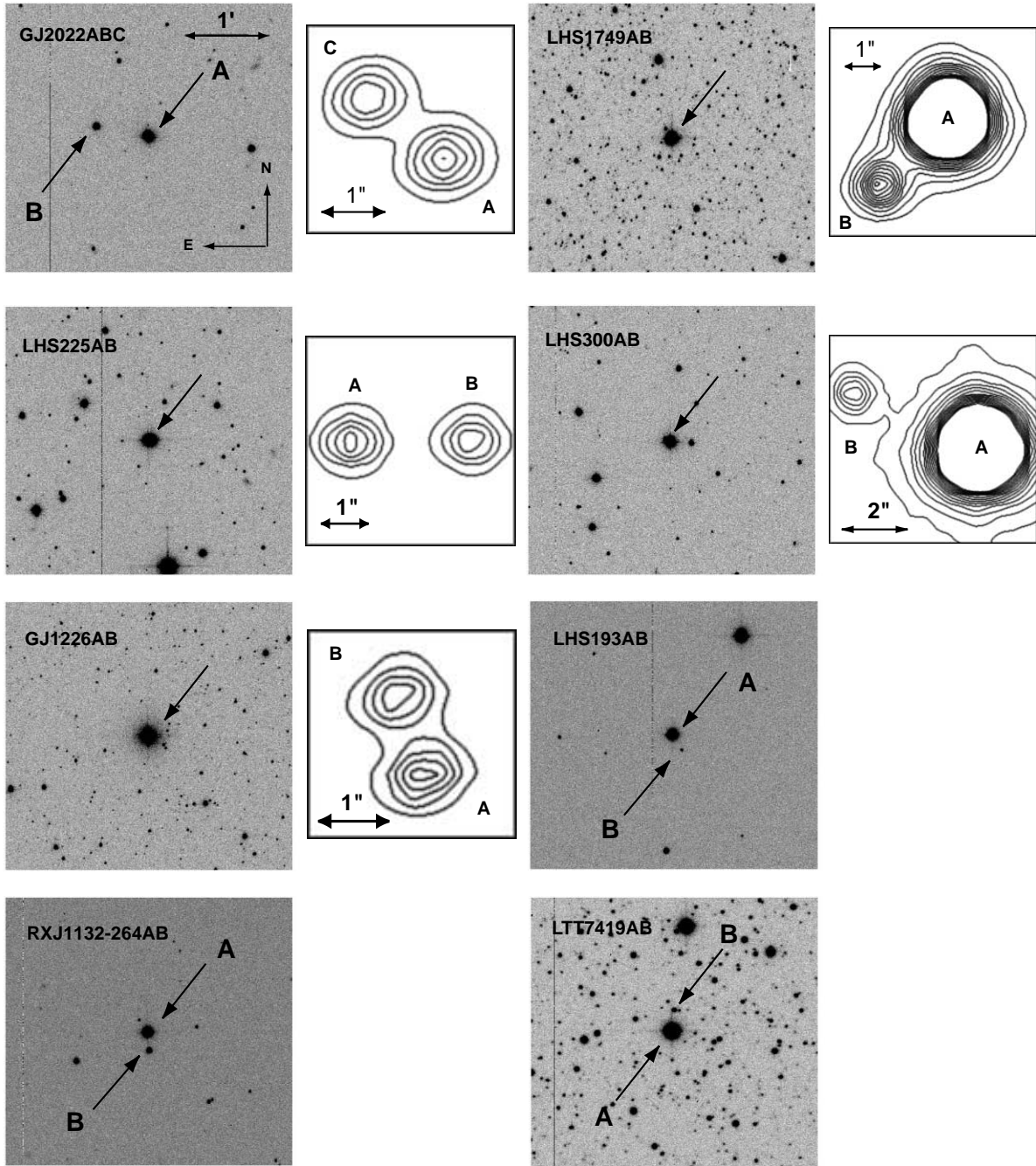


FIG. 1.—Eight new companions found in CTIOPI images. Each finder image is cut from a CTIOPI frame and is $3/3 \times 3/3$, with north up and east to the left. Insets show the contour maps from the IRAF IMEXAMINE task. Companions to LHS 193, RX J1132–264 and LTT 7419 are obvious in the CTIOPI frames.

in CTIOPI, the average FWHM for the brightest nonsaturated objects in the field is $6''.65$ —this is a “best case” estimate for saturated stars, for which the resolution limit is typically much worse.

The detection limit of the CTIOPI frames is compared with that of DSS in Figure 3. Four CTIOPI objects were used as benchmarks for this illustration—two each with FWHM values matching the best ($0''.85$; *filled triangles and circles*) and worst ($1''.20$; *open triangles and circles*) seeing cases for the bulk of the sample, as shown in Figure 2. For these four targets, objects of varying magnitude differences were selected from the same frames searched forcompan-

ions and artificially placed at increasing separations from the target stars in increments of $0''.40$ (1 pixel). The points in Figure 3 represent the closest separation at which the simulated companion could be detected using the methodology described above. The same procedure was carried out on a DSS image (*filled squares*) for an unsaturated program star. Clearly, five of the eight new companion candidates (*large starred points*) were undetectable in DSS images but are clearly resolved in CTIOPI images. However, LHS 193B, LTT 7419B, and RX J1132–264B are at large separations from their primary stars and can be seen in DSS images. They were simply unnoticed before.

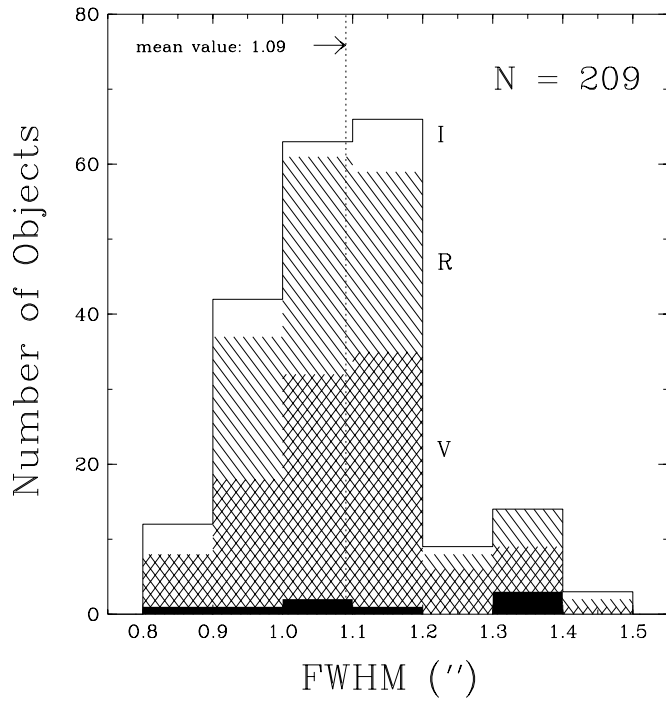


FIG. 2.—Histogram showing the FWHM of images used to search 209 stars for new companions. The mean FWHM is $1''\!09$, and 87% of the stars have $\text{FWHM} < 1''\!2$. Stars searched using V , R , and I filters are indicated by crosshatching, hatching, and white space, respectively. The dark bars represent the eight new companions.

3.3. Astrometric Confirmation of New Multiple Systems

Two methods were used to confirm or refute the eight potential companions, as well as to check the validity of 17 previously cataloged companions. First, the relative positions of the target stars and their potential companions were mapped using the series of astrometric frames in hand. This technique was used to check for constant relative positions and slow orbital motion. Second, full astrometric analyses were carried out to determine if multiple components had common proper motion. Series of astrometric frames were analyzed with SExtractor and a modified version of the University of Virginia parallax reduction pipeline (to be discussed in a future paper) to determine precise relative separations and position angles and, ultimately, proper-motion vectors.

To map the relative position of a potential companion over time, first a reference trail frame is selected from the parallax series. All other frames must be adjusted to match the trail frame in scale, rotation, and translation. The trail frame is chosen to have (1) correct orientation to the sky (i.e., north-south and east-west directions properly aligned on the CCD chip), (2) sufficient S/N in the target star and all reference stars to permit reliable centroids, and (3) a very short right ascension zenith distance (within $10'$ of the meridian) to reduce differential refraction effects.

A six-constant plate model is then applied to each frame to provide sets of modified coordinates for the target star(s) and any potential companions, using the methodology outlined by Eichhorn & Jefferys (1971) and Jefferys (1979) and

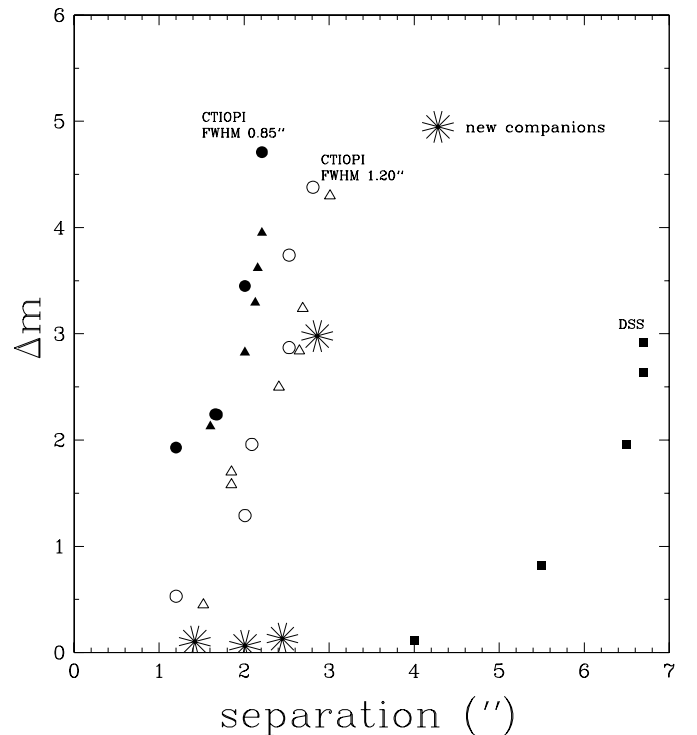


FIG. 3.—Schematic illustrating the magnitude difference limits (in the primary astrometry filter for each star) reached between companions and targets at various separations. Circles and triangles represent the closest separations at which simulated companions could be detected in CTIOPI frames, using two frames with excellent seeing ($0''\!85$, *filled points*) and two frames with poor seeing ($1''\!20$, *open points*). Simulated companions to targets in DSS images are represented by filled squares. Five of the eight new companions discovered are plotted as starred points. Their positions on the plot demonstrate that increased-resolution CTIOPI images were necessary for their discovery.

described by the following equations:

$$\xi = X' - aX + bY + c, \quad (1)$$

$$\eta = Y' - dX + eY + f, \quad (2)$$

where X and Y are the coordinates for science and reference stars on the CCD chip that are extracted from SExtractor. X' and Y' are the coordinates on the reference trail frame. The plate constants a , b , c , d , e , and f model the coordinate scales in X and Y , rotation, and translation. An iterative least-squares technique is carried out to reduce the differences between the trail plate and the plate examined, resulting in minimized values of ξ and η .

The separation and position angle are then computed for each frame at multiple epochs for a target-companion pair and plotted as in Figure 4 for LHS 225 AB. The solid lines indicate the best fit for the separation and position angle for LHS 225 AB at six epochs. If component B were a stationary field star that held its location at the first epoch of observation, its separation and position angle relative to the primary would change, as indicated by the dot-dashed lines. Clearly, LHS 225B maintains a constant separation and position angle throughout the 1.2 yr baseline of our observations. All eight potential companions have been confirmed using this method, as well as 16 previously known companions.

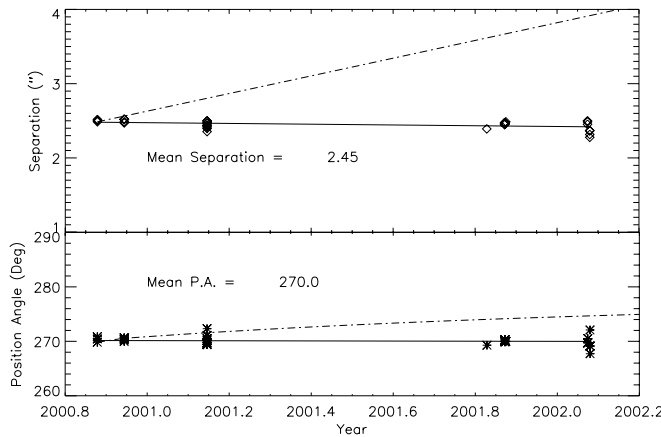


FIG. 4.—Example companion confirmation plot illustrating that the new component LHS 225B is physically associated with the primary star. The solid lines in the two panels mark the fits for position angle and separation. The dot-dashed line represents the relative motion of B to the primary star if it were a field star.

Orbital motion would be detected if the best-fit line varied from a constant value (either a tilted or a curved line, depending on orbital velocity). However, no orbital motion was detected for any of the new close companions, even for GJ 1226 AB, which has the smallest separation ($1.^{\circ}42$). Figure 5 illustrates the relative positions for the five new multiple systems with separations less than $5''$. Note that at smaller separations the centroid positions are more scattered, which results in relatively large errors in the four astrometric quantities derived. The results of these fits for mean separation and position angle are given in Table 2 (cols. [2] and [3]), and the timescale over which the frames were taken is given in the last column.

For each system, a second verification of true companionship was carried out by determining the proper-motion vectors for the primaries and all companions. The model used

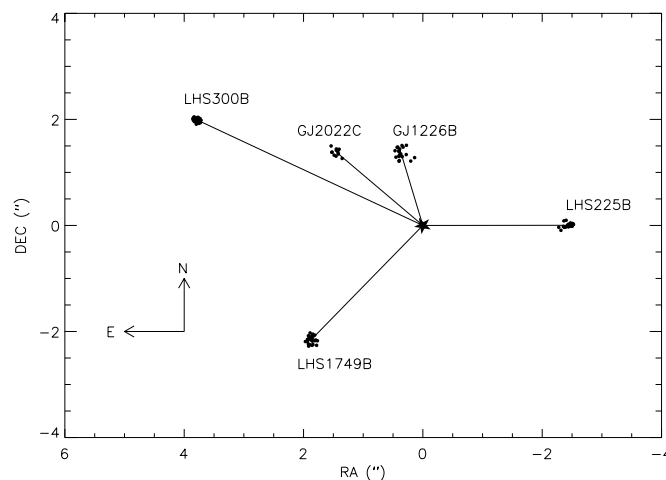


FIG. 5.—Five new companions with separations less than $5''$. The star symbol marks the position of each system's primary. Note that with increasing separation, the centroid is more concentrated, indicating that centroiding accuracy increases at larger separations. The three widely separated new binary systems, LHS 193 AB, RX J1132–262 AB, and LTT 7419 AB, are not shown in this figure. North is up, and east is to the left.

is from van de Kamp (1967),

$$\xi = X' - (c_x + P_x \pi_x + \mu_x t), \quad (3)$$

$$\eta = Y' - (c_y + P_y \pi_y + \mu_y t), \quad (4)$$

where X' and Y' are the modified coordinates in right ascension and declination, P_x and P_y are the parallax factors, π_x and π_y are relative trigonometric parallaxes, μ_x and μ_y are relative proper motions, and t is the fractional year for each frame. The variables c_x and c_y are constant. Subscripts x and y are for quantities in right ascension and declination, respectively. Parallax factors P_x and P_y for each frame are calculated from the Naval Observatory Vector Astrometry Subroutines, SOLSYS.³ As before, a least-squares method is applied to produce the relative proper motions by minimizing the values of ξ and η .

Each of the eight new candidate companions has proper motions that are consistent in both magnitude and direction with their primaries, confirming that all companion candidates are true companions. Results of the astrometric solutions for proper motion and position angle are shown in Table 2 (cols. [4] and [5]), for 21 true multiple systems. Note a indicates the eight new companions. Full analyses, including parallaxes, await acquisition of final frames in the astrometric series. Typical errors are less than 20 mas yr^{-1} for the proper motions and less than 5° for the position angles. Larger errors occur in cases where the system is a close multiple (LHS 1749, LHS 225, and GJ 1226) or the secondary is quite faint (LHS 193). The complicated GJ 2022 ABC system has limited data resulting in large errors, as discussed in § 5. The time series for BD $-21^\circ 1074$ ABC and LTT 9123 AB are insufficient for reliable proper-motion determinations.

HIP 82724 and HIP 82725 have the largest statistically different proper motions (4.0σ) of the systems observed, implying that they are not physically associated. The high errors in the proper-motion position angles are the result of very small proper motions, which makes the direction of the motion difficult to determine. Based on our own spectroscopic observations taken at the CTIO 4 m telescope in 2002 April, we confirm that the two stars are not a physical pair—HIP 82725 is a giant, and HIP 82724 is a dwarf, yet they have similar magnitudes, with $V = 11.72$ and $V = 11.85$, respectively.

4. DATA REDUCTION AND ANALYSIS: DIFFERENTIAL PHOTOMETRY

Differential photometry between the primary stars and the 23 true companions was measured using all available frames at V_J , R_C , and I_C filters. In addition to evaluating the colors of the components, the rich data sets available provide an opportunity to search for both long-term (a few years) and short-term (a few minutes) variability. Typically, a system is observed only once per observing run for astrometry, so the current data sets do not provide insight into variability on timescales of a few nights.

Extractor was used to determine the fluxes for all resolvable components in each system. For components with separations less than $10''$, a $1''$ radius aperture was used to prevent the Moffat profile wings from overlapping, which

³ Available at <http://aa.usno.navy.mil/software/>.

TABLE 2
ASTROMETRY DATA FOR CTIOPI RESOLVED SYSTEMS

Object Name (1)	Separation (arcsec) (2)	P.A. of Component (deg) (3)	μ (arcsec yr ⁻¹) (4)	P.A. of μ (deg) (5)	No. of Epochs (6)	Time Coverage (year fraction) (7)
G266-089A	1.383 ± 0.006	192.2 ± 0.4		
G266-089B	9.02 ± 0.01	321.08 ± 0.02	1.388 ± 0.007	192.0 ± 0.5	5	2000.87–2001.87
GJ 2006A	0.117 ± 0.005	101.2 ± 4.4		
GJ 2006B	17.87 ± 0.01	175.02 ± 0.08	0.100 ± 0.006	106.5 ± 4.5	5	2000.57–2001.83
GJ 2022A	0.239 ± 0.048	126.9 ± 21.9		
GJ 2022B	37.84 ± 0.05	78.53 ± 0.07	0.179 ± 0.016	129.2 ± 9.8		
GJ 2022C ^a	2.01 ± 0.07	46.38 ± 1.31	0.303 ± 0.068	128.2 ± 23.8	5	1999.62–2000.87
G274-138A	0.344 ± 0.008	147.8 ± 2.5		
G274-138B	3.59 ± 0.01	60.40 ± 0.17	0.344 ± 0.009	146.5 ± 2.9	6	2000.57–2001.75
LP 993-115 (A)	0.386 ± 0.003	174.5 ± 0.7		
LP 993-116 (B)	44.55 ± 0.02	61.09 ± 0.01	0.372 ± 0.003	172.8 ± 0.7	6	1999.62–2001.95
LP 771-095 (A)	0.475 ± 0.004	234.5 ± 1.0		
LP 771-096 (BC)	7.22 ± 0.03	315.06 ± 0.05	0.484 ± 0.004	238.7 ± 1.0	3	1999.64–2001.75
LHS 193A	1.016 ± 0.007	45.2 ± 0.8		
LHS 193B ^a	12.59 ± 0.05	210.67 ± 0.21	1.013 ± 0.031	41.3 ± 3.4	5	2000.87–2002.08
LT T 2043 (A)	0.339 ± 0.005	238.4 ± 1.6		
LT T 2044 (B)	49.58 ± 0.01	195.97 ± 0.01	0.333 ± 0.006	238.8 ± 2.1	5	2000.88–2002.08
BD -21°1074A		
BD -21°1074 BC	8.22 ± 0.01	311.18 ± 0.16	2	
LHS 1749A	0.811 ± 0.008	355.7 ± 0.7		
LHS 1749B ^a	2.86 ± 0.06	139.02 ± 1.11	0.798 ± 0.038	355.8 ± 3.7	5	2000.88–2002.08
LHS 225A	1.267 ± 0.023	102.5 ± 1.5		
LHS 225B ^a	2.45 ± 0.06	270.06 ± 0.81	1.208 ± 0.020	102.4 ± 1.3	6	2000.88–2002.08
LHS 2067 (A)	0.632 ± 0.002	75.4 ± 0.3		
LHS 2068 (B)	18.23 ± 0.02	89.28 ± 0.05	0.627 ± 0.006	77.1 ± 0.9	8	2000.14–2002.29
LT T 3790 (A)	0.213 ± 0.017	188.5 ± 2.7		
LT T 3791 (B)	30.91 ± 0.01	119.82 ± 0.01	0.212 ± 0.017	188.7 ± 3.0	4	2000.14–2002.07
LHS 300A	1.253 ± 0.003	264.0 ± 0.2		
LHS 300B ^a	4.28 ± 0.04	62.27 ± 0.41	1.257 ± 0.016	264.3 ± 1.0	5	2001.15–2002.29
RX J1132–264A	0.073 ± 0.002	255.4 ± 2.9		
RX J1132–264B ^a	13.18 ± 0.01	185.49 ± 0.04	0.072 ± 0.003	255.1 ± 4.0	6	2000.14–2002.29
LHS 2567 (A)	0.599 ± 0.002	241.6 ± 0.4		
LHS 2568 (B)	7.94 ± 0.01	60.96 ± 0.04	0.591 ± 0.002	242.1 ± 0.4	4	2000.07–2002.44
LHS 3001 (A)	0.972 ± 0.003	301.1 ± 0.4		
LHS 3002 (B)	12.67 ± 0.02	45.46 ± 0.05	0.989 ± 0.005	300.7 ± 0.5	6	2000.58–2002.28
HIP 82725	0.006 ± 0.003	62.2 ± 45.3		
HIP 82724 ^b	12.97 ± 0.01	109.09 ± 0.22	0.055 ± 0.012	63.7 ± 17.0	7	2000.23–2002.53
GJ 2130 AC	0.278 ± 0.002	195.6 ± 0.5		
GJ 2130B	21.23 ± 0.01	88.22 ± 0.01	0.278 ± 0.002	196.2 ± 0.5	7	1999.64–2002.44
GJ 1226A	1.146 ± 0.031	214.2 ± 3.0		
GJ 1226B ^a	1.42 ± 0.09	14.99 ± 3.13	1.213 ± 0.046	211.1 ± 4.3	4	2000.57–2001.60
LT T 7419A	0.387 ± 0.003	200.3 ± 0.7		
LT T 7419B ^a	14.90 ± 0.02	353.83 ± 0.12	0.394 ± 0.006	204.1 ± 1.6	9	2000.57–2002.57
LHS 501 (A)	1.493 ± 0.002	107.9 ± 0.1		
LHS 500 (B)	107.12 ± 0.02	185.18 ± 0.03	1.488 ± 0.002	108.3 ± 0.2	8	1999.71–2002.44
LHS 3739 (A)	0.535 ± 0.006	228.2 ± 1.2		
LHS 3738 (B)	113.15 ± 0.03	353.30 ± 0.01	0.540 ± 0.005	226.7 ± 1.0	3	1999.64–2002.51
LT T 9123 (A)		
LT T 9124 (B)	14.57 ± 0.01	136.24 ± 0.04	2	

^a New companion.^b Refuted companion.

would corrupt the relative counts and derived magnitude differences. A 5'' radius aperture was used for systems with separations greater than 10'', except in the case of LT T 7419, for which a 1'' aperture was used because of a faint background star near to component B.

Brightness ratios for each filter were derived using simple ratios of the total counts included in the apertures, i.e., point-spread function fits were not done. Instrumental magnitude differences were determined using the usual conver-

sion of brightness ratio to magnitude difference, and the results are listed in Table 3 (col. [6]). Because standard stars on the Johnson and Cousins systems were not (yet) observed, the magnitude differences listed are slightly different from what will be available when full photometric calibrations have been done. Of the 23 companions examined, six have a magnitude difference greater than 2.5 in the primary filter, making these companions more than 10 times fainter than their primaries. LT T 7419 AB has the largest

TABLE 3
MAGNITUDE DIFFERENCES FOR CTIOPI RESOLVED SYSTEMS

Object Name (1)	Aperture ^a (arcsec) (2)	Filter (3)	No. of Frames (4)	No. of Nights (5)	Δm (6)	Nightly Error ^b (7)
G266-089 AB.....	1	<i>V</i>	30	6	0.552 ± 0.006	0.001–0.005
		<i>R</i>	6	2	0.512	0.001
		<i>I</i>	6	2	0.420	0.003
GJ 2006 AB.....	5	<i>V</i>	22	4	0.266 ± 0.084	0.001–0.002
		<i>R</i>	5	2	0.304	0.000
		<i>I</i>	6	2	0.210	0.001
GJ 2022 AB.....	1	<i>V</i>	8	3	1.315 ± 0.039	0.012–0.026
		<i>R</i>	13	6	1.174 ± 0.046	0.003–0.013
		<i>I</i>	5	2	1.063	0.019
GJ 2022 AC ^c	1	<i>V</i>	8	2	0.064	0.042
		<i>R</i>	13	6	0.095 ± 0.037	0.008–0.026
		<i>I</i>	5	2	0.076	0.003
G274-138 AB.....	1	<i>I</i>	41	7	0.117 ± 0.004	0.003–0.010
LP 993-115 AB.....	5	<i>V</i>	35	7	0.338 ± 0.023	0.002–0.011
		<i>R</i>	1	1	0.224	...
		<i>I</i>	1	1	0.067	...
LP 771-095 A-BC.....	1	<i>V</i>	28	5	0.304 ± 0.050	0.007–0.041
		<i>R</i>	1	1	0.124	...
		<i>I</i>	4	1	-0.035	0.017
LHS 193 AB ^c	5	<i>V</i>	34	6	5.933 ± 0.035	0.017–0.123
LTT 2043 AB.....	5	<i>V</i>	38	6	0.285 ± 0.007	0.001–0.002
		<i>I</i>	2	1	0.197	0.006
		<i>V</i>	15	2	0.722	0.007–0.014
BD -21°1074 A-BC	1	<i>R</i>	5	1	0.574	0.005
		<i>I</i>	8	2	0.220	0.004–0.006
		<i>V</i>	30	7	2.979 ± 0.124	0.026–0.161
LHS 1749 AB ^c	1	<i>V</i>	35	8	0.131 ± 0.012	0.005–0.016
		<i>R</i>	6	5	0.126 ± 0.013	0.003
		<i>I</i>	3	2	0.108	0.003
LHS 2067 AB.....	5	<i>I</i>	47	13	3.231 ± 0.020	0.003–0.047
LTT 3790 AB.....	5	<i>V</i>	37	5	1.533 ± 0.002	0.001–0.004
		<i>R</i>	1	1	1.347	...
		<i>I</i>	1	1	0.969	...
LHS 300 AB ^c	1	<i>V</i>	1	1	4.667	...
		<i>R</i>	32	6	4.948 ± 0.063	0.005–0.112
		<i>I</i>	1	1	4.972	...
RX J1132–264 AB ^c	5	<i>V</i>	38	6	2.978 ± 0.168	0.003–0.143
		<i>R</i>	5	1	2.613	0.003
		<i>I</i>	5	1	1.993	0.005
LHS 2567 AB.....	1	<i>V</i>	5	1	1.149	0.002
		<i>R</i>	27	5	1.113 ± 0.007	0.003–0.016
		<i>I</i>	5	1	1.054	0.009
LHS 3001 AB.....	5	<i>V</i>	7	2	3.130	0.040–0.075
		<i>R</i>	5	2	2.460	0.006–0.011
		<i>I</i>	46	9	1.922 ± 0.009	0.002–0.013
GJ 2130 AC-B.....	5	<i>V</i>	47	8	0.997 ± 0.016	0.001–0.005
		<i>R</i>	14	3	0.845 ± 0.007	0.005–0.008
		<i>I</i>	14	3	0.531 ± 0.006	0.001–0.008
GJ 1226 AB ^c	1	<i>V</i>	8	2	0.157	0.027–0.197
		<i>R</i>	9	2	0.106	0.090–0.094
		<i>I</i>	33	6	0.103 ± 0.035	0.032–0.070
LTT 7419 AB ^c	1	<i>V</i>	60	9	6.065 ± 0.036	0.008–0.021
		<i>R</i>	1	1	5.315	...
		<i>I</i>	1	1	4.393	...
LHS 501 AB.....	5	<i>V</i>	83	14	2.129 ± 0.017	0.001–0.008
		<i>R</i>	5	1	1.987	0.005
		<i>I</i>	5	1	1.780	0.005
LHS 3739 AB.....	5	<i>V</i>	5	1	1.054	0.004
		<i>R</i>	21	4	0.850 ± 0.008	0.001–0.004
		<i>I</i>	10	2	0.580	0.001–0.003
LTT 9123 AB.....	5	<i>V</i>	15	3	1.717 ± 0.005	0.001–0.003
		<i>R</i>	11	2	1.576	0.002–0.003
		<i>I</i>	10	2	1.319	0.002–0.003

^a Radius within which the flux was obtained for each component.

^b Range of errors from individual nights.

^c New companion in system.

magnitude difference observed, $\Delta V = 6.06$. The disparity between the number of frames and nights per filter for a given system (cols. [4] and [5] of Table 3) arises because the bulk of frames taken are in a single filter for the astrometry program, while the other two filters are acquired only for relative or absolute photometry.

The errors on the magnitude differences were derived by taking the standard deviation of the nightly means, e.g., using six values for G266-089 AB, not 30 values, corresponding to the number of frames. A closer look at these errors provides a hint of the long-term variability in each system. The timescale over which long-term variability might be detected ranges from ~ 1.0 to 2.5 yr, as listed in final column of Table 2. One exception to these timescales is the new close binary, GJ 1226 AB, for which fewer frames were available for astrometry than for variability. In many images the components were blended, making accurate centroid measurements impossible. However, flux ratios were obtainable from many of these blended frames, yielding a variability baseline of 2000.57–2002.46.

Shown in Figure 6 are the magnitude difference errors in the primary filters plotted as a function of separation for the 23 companions (BD-21°1074 ABC is not plotted, because no reliable error can be deduced from only two nights of data). Companions more than 2.5 mag fainter than their primaries are shown as circled points. Only four companions have $\sigma_{\Delta m} > 0.05$, which is selected as a rather conservative variability threshold. Of these, LHS 1749 AB has a small separation (2''.86) and a large $\Delta V = 2.98$, which conspire to cause a large measurement error unrelated to variability. LHS 300 AB also has a relatively small separation (4''.28) and large $\Delta R = 4.95$, again resulting in a large measurement error. RX J1132-264 AB is a wide binary (13''.18),

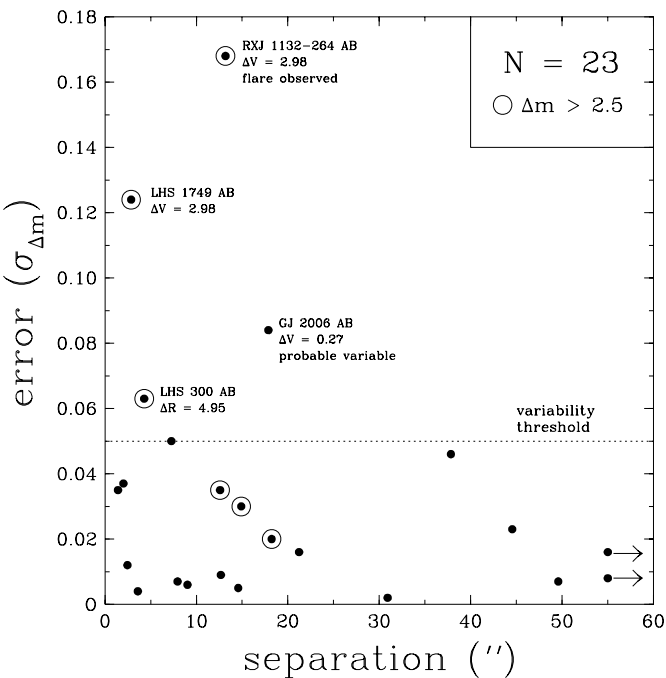


FIG. 6.—Errors in the magnitude differences between 23 companions and their primaries plotted vs. separation. Open circles indicate a magnitude difference greater than 2.5. RX J1132–264 AB is a flare system, and GJ 2006 AB is likely a variable system. Because of their large separations, LHS 501 AB and LHS 3739 AB are not plotted to scale but are shown at bottom right with arrows.

and the series of $\Delta V = 2.98, 3.00, 2.55, 2.99, 3.10$, and 3.12 values are relatively consistent except for the third epoch (discussed below), hinting at some sort of variability. Finally, there is compelling evidence for long-term variability in GJ 2006 AB, which is widely separated ($17''.87$) and has a small $\Delta V = 0.27$, with measurements at four epochs of $\Delta V = 0.21, 0.17, 0.39$, and 0.29 . Comparison of both components to a field star indicates that both A and B may be variable. The errors for the remaining systems indicate that the typical measurement accuracy for magnitude differences during CTIOPI is a few hundredths of a magnitude.

A search for short-term variability, indicated by the error in a single night's measurements, is possible because several frames are usually taken on a system each night. The range of nightly errors for each system is given in the last column of Table 3. Examining the rich data sets taken in the primary parallax filters reveals five companions that have at least one night on which the error is greater than 0.05 mag. As before, in most cases (LHS 193 AB, LHS 1749 AB, LHS 300 AB, and GJ 1226 AB), the large errors can be attributed to small separations and/or large Δm . RX J1132-264 AB is the standout. The B component shows a flare event on 2000 April 18 that leads to a large error on that night, which is the single night with a very different ΔV value mentioned above. The series of four sequential frames yields $\Delta V = 2.31, 2.60, 2.63$, and 2.65 , revealing a significant spike in component B's luminosity at the beginning of the series, which is likely a flare caught near its peak.

5. NOTES ON INDIVIDUAL SYSTEMS

The following stars (listed in alphabetical order) are worthy of special note.

GJ 2005 ABC is noticeably elongated. Although they are not resolved, the faint B and C components are blended into a single bump to the north of the primary.

GJ 2006 AB contains at least one long-term variable star. The large error in the proper motion position angle is caused by the small total proper motion in only 1.26 yr. Furthermore, there are only five faint reference stars, resulting in a weak astrometric field and the consequent high errors in proper-motion position angle.

GJ 2022 ABC has a new third component 2.01 from A with $\Delta R = 1.2$. Among 38 images, there are only 13 images in which A and C are resolved. Of these, 11 images were taken between 1999.6 and 1999.9, and only two images were taken on 2000.8. Therefore, the spotty coverage in the series yields a relatively poor astrometric solution. More images are expected in the future to improve the results.

LHS 300 AB is a new binary with very different components ($\Delta R = 4.9$) separated by 4."28 in a system of high proper motion, 1."2 yr. The secondary is a white dwarf, as is indicated by its color relative to A and supported by spectroscopic data acquired in 2002 April.

LT Tauri 7419 AB has a new companion with the largest magnitude difference ($\Delta V = 6.1$) and separation (14''.90) found among the new multiples. The colors of the companion indicate that it is a white dwarf.

RX J1132-264 AB includes a new companion that was caught flaring in one sequence of frames. This system is a known X-ray source (Fleming 1998), but this is the first identification of the flaring companion.

6. STELLAR MULTIPLICITY AND VARIABILITY RATES

Research on stellar multiplicity indicates that the multiplicity fraction is dependent on spectral type. Mason et al. (1998) found that more than 59% of O-type stars in clusters and associations have a visual, speckle, or spectroscopic companion. Duquennoy & Mayor (1991) found that 65% of solar-type primaries have companions with masses greater than $0.01 M_{\odot}$. The multiplicity fraction drops to 34%–42% for the M dwarfs, as found by Henry & McCarthy (1990) and Fischer & Marcy (1992).

Most of the primary stars in the 191 systems examined in this study are M dwarfs. The census for this sample now includes 21 doubles and seven triples, bringing the multiplicity fraction to 15%. Given that most of these stars are potential, but not known, nearby M dwarfs in the southern sky, few have been observed in any significant way until CTIOPI, so the multiplicity fraction is certainly greater than observed to date. Many would undoubtedly be revealed to be multiples in future high-resolution imaging or radial velocity surveys. With modern techniques such as high-resolution interferometry, like the CHARA Array, we expect not only to discover more multiple systems, but to map their orbits accurately enough to determine precise masses. In addition, we expect to find several as yet unidentified companions by carefully determining the residuals from our trigonometric parallax reductions, in a similar fashion to the significant work of van de Kamp (1986).

Of the 23 companions observed for variability, one was determined to be a long-term variable and one was observed to flare. This 9% hit rate for red dwarf variability is much lower than the long-term study of 43 (generally single) M dwarfs observed by Weis (1994), who found a variability fraction of 49% using absolute photometry, rather than relative photometry. However, the present work has a much shorter time baseline (1.0–2.5 yr compared with Weis's 11 yr survey) and has a more restrictive criterion for variability (0.05 mag compared with ~ 0.01 for Weis). Presumably, with further observations many of the companions in this

study would be found to be variable at a lower level than the threshold adopted.

7. FUTURE

Given our success in finding the new companions reported here and the discovery of many new nearby stars indicated by our preliminary parallax results (to be published in future papers), we are poised to continue filling in the nearby-star census via CTIOPI. In addition to providing a more complete picture of the Sun's neighbors, CTIOPI results will also provide targets for upcoming space missions such as *SIM* (the *Space Interferometry Mission*) and *TPF* (*Terrestrial Planet Finder*), which can observe many of these nearby stars to determine precise stellar masses in the binaries, look for perturbations caused by planets in the binaries, and search the single stars for planetary systems.

We are grateful to Alberto Miranda and the staff at the National Science Foundation's Cerro Tololo Inter-American Observatory, in particular Edgardo Cosgrove, Manuel Hernandez, and Alistair Walker, for their assistance during this long-term program at the CTIO 0.9 m telescope. We also thank Jennifer Bartlett for her recent work on CTIOPI. Of course, this science would not be possible without the generous support of the NOAO Surveys Program. The Georgia State and University of Virginia teams benefit from support by NASA's Nearby Stars (NSTars) Project (<http://nstars.arc.nasa.gov>) and NASA's *Space Interferometry Mission*. The Chilean team acknowledges support from the Fondo Nacional de Investigación Científica y Tecnológica (FONDECYT project 1010137). E. C. also acknowledges support from the Chilean Centro de Astrofísica (FONDAP No. 15010003). This research has made use of the SIMBAD database, operated at CDS, Strasbourg, France. More information on RECONS work is available at <http://www.chara.gsu.edu/RECONS>.

REFERENCES

- Abt, H. A., & Levy, S. G. 1976, ApJS, 30, 273
- Albrecht, M. A., Brighton, A., Herlin, T., Biereichel, P., & Durand, D. 1997, in ASP Conf. Ser. 125, Astronomical Data Analysis Software and Systems VI, ed. G. Hunt & H. E. Payne (San Francisco: ASP), 333
- Bakos, G. A., Sahu, K. C., & Németh, P. 2002, ApJS, 141, 187
- Bertin, E., & Arnouts, S. 1996, A&AS, 117, 393
- Delfosse, X., Forveille, T., Beuzit, J.-L., Udry, S., Mayor, M., & Perrier, C. 1999, A&A, 344, 897
- Duquennoy, A., & Mayor, M. 1991, A&A, 248, 485
- Eichhorn, H., & Jefferys, W. H. 1971, Publ. Leander McCormick Obs., 16, 267
- Fischer, D. A., & Marcy, G. W. 1992, ApJ, 396, 178
- Fleming, T. A. 1998, ApJ, 504, 461
- Henry, T. J. 1991, Ph.D. thesis, Univ. Arizona
- Henry, T. J., Ianna, P. A., Kirkpatrick, J. D., & Jahreiss, H. 1997, AJ, 114, 388
- Henry, T. J., & McCarthy, D. W., Jr. 1990, ApJ, 350, 334
- Hinz, J. L., McCarthy, D. W., Jr., Simons, D. A., Henry, T. J., Kirkpatrick, J. D., & McGuire, P. C. 2002, AJ, 123, 2027
- Jefferys, W. H. 1979, AJ, 84, 1775
- Leinert, C., Henry, T. J., Glindemann, A., & McCarthy, D. W., Jr. 1997, A&A, 325, 159
- McCarthy, C., Zuckermann, B., & Becklin, E. E. 2001, AJ, 121, 3259
- Marcy, G. W., & Benitz, K. J. 1989, ApJ, 344, 441
- Mason, B. D., Gies, D. R., Hartkopf, W. I., Bagnuolo, W. G., Jr., ten Brummelaar, T., & McAlister, H. A. 1998, AJ, 115, 821
- Poveda, A., Herrera, M. A., Allen, C., Cordero, G., & Lavalle, C. 1994, Rev. Mexicana Astron. Astrofis., 28, 43
- Scholz, R.-D., Irwin, M. J., Ibata, R., Jahreiss, H., & Malkov, O. Yu. 2000, A&A, 353, 958
- Simons, D. A., Henry, T. J., & Kirkpatrick, J. D. 1996, AJ, 112, 2238
- Skrutskie, M. F., Forrest, W. J., & Shure, M. A. 1989, AJ, 98, 1409
- van Biesbroeck, G. 1961, AJ, 66, 528
- van de Kamp, P. 1967, Principles of Astrometry (San Francisco: Freeman)
- . 1986, Space Sci. Rev., 43, 211
- Weis, E. W. 1994, AJ, 107, 1135